University of Massachusetts Medical School

eScholarship@UMMS

2020-11-17

Poly(A)-Binding Protein Regulates the Efficiency of Translation Termination

Chan Wu
University of Massachusetts Medical School

Et al.

Let us know how access to this document benefits you.

Follow this and additional works at: https://escholarship.umassmed.edu/oapubs

Part of the Amino Acids, Peptides, and Proteins Commons, Biochemistry, Biophysics, and Structural Biology Commons, Cellular and Molecular Physiology Commons, and the Nucleic Acids, Nucleotides, and Nucleosides Commons

Repository Citation

Creative Commons License

Poly(A)-Binding Protein Regulates the Efficiency of Translation Termination

Graphical Abstract

Readthrough Termination

Highlights

- Premature translational termination manifests position effects in yeast mRNAs

- Termination increases and readthrough decreases as stop codons approach the ORF 3′ end

- Stop codon proximity to 3′ poly(A)-binding protein regulates termination efficiency

- Positional variation and termination dependence on Pab1 support an NMD *faux*-UTR model

Authors

Chan Wu, Bijoyita Roy, Feng He,
Kevin Yan, Allan Jacobson

Correspondence

allan.jacobson@umassmed.edu

In Brief

Premature termination codons (PTCs) trigger translational termination and can promote mRNA decay. Wu et al. insert PTCs at multiple locations in yeast genes and find that their termination efficiencies increase with proximity to ORF 3′ ends and that this positional effect on termination is modulated through mRNA-associated poly(A)-binding protein.

Cell Reports

Report

Poly(A)-Binding Protein Regulates the Efficiency of Translation Termination

Chan Wu,[1] Bijoyita Roy,[1,2] Feng He,[1] Kevin Yan,[1,3] and Allan Jacobson[1,4,*]
[1]Department of Microbiology and Physiological Systems, University of Massachusetts Medical School, 368 Plantation Street, Worcester, MA 01655, USA
[2]Present address: New England Biolabs, 240 County Road, Ipswich, MA 01938, USA
[3]Present address: Yale School of Medicine, Department of Neurology, 20 York Street, LLCI 912, New Haven, CT 06510, USA
[4]Lead Contact
*Correspondence: allan.jacobson@umassmed.edu
https://doi.org/10.1016/j.celrep.2020.108399

SUMMARY

Multiple factors influence translation termination efficiency, including nonsense codon identity and immediate context. To determine whether the relative position of a nonsense codon within an open reading frame (ORF) influences termination efficiency, we quantitate the production of prematurely terminated and/or readthrough polypeptides from 26 nonsense alleles of 3 genes expressed in yeast. The accumulation of premature termination products and the extent of readthrough for the respective premature termination codons (PTCs) manifest a marked dependence on PTC proximity to the mRNA 3′ end. Premature termination products increase in relative abundance, whereas readthrough efficiencies decrease progressively across different ORFs, and readthrough efficiencies for a PTC increase in response to 3′ UTR lengthening. These effects are eliminated and overall translation termination efficiency decreases considerably in cells harboring *pab1* mutations. Our results support a critical role for poly(A)-binding protein in the regulation of translation termination and also suggest that inefficient termination is a trigger for nonsense-mediated mRNA decay (NMD).

INTRODUCTION

Translation termination in eukaryotes is orchestrated by the release factors eRF1 and eRF3 when any of the three stop codons (UAA, UAG, or UGA) in an mRNA occupies the A site of a ribosome (Alkalaeva et al., 2006; Stansfield et al., 1995; Zhouravleva et al., 1995). eRF1 recognizes A-site-localized stop codons and hydrolyzes peptidyl-tRNA, whereas eRF3 interacts with eRF1 and stimulates termination by its GTPase activity (Alkalaeva et al., 2006; Salas-Marco and Bedwell, 2004). eRF1 and nearcognate tRNAs (nc-tRNAs), i.e., tRNAs capable of base pairing with stop codons at two of the three standard codon positions, compete for binding to the ribosomal A site (Brown et al., 2015). Although this competition is inefficient for nc-tRNA, when successful, it leads to the insertion of an amino acid and continuation of translational elongation until the next in-frame stop codon is encountered (Roy et al., 2015, 2016). Such a bypass of translation termination is designated nonsense suppression or readthrough (Brenner et al., 1965; Keeling et al., 2014; Peltz et al., 2013).

Multiple factors appear to influence the competition between nc-tRNAs and eRF1 and, hence, the extent of nonsense suppression, including (1) the identity of the stop codon, with UGA promoting higher levels of readthrough than UAG or UAA (Howard et al., 2000; Loughran et al., 2014; Manuvakhova et al., 2000); (2) the immediate context of a stop codon, with the highest readthrough levels typically occurring when adenine precedes and cytosine follows the stop codon (Bonetti et al., 1995; McCaughan

et al., 1995; Mottagui-Tabar et al., 1998; Tork et al., 2004); (3) specific sequences or structures 3′ to the stop codon (Anzalone et al., 2019; Cridge et al., 2018; Harrell et al., 2002; Namy et al., 2001; Skuzeski et al., 1991); and (4) the integrity of the release factors and the ribosome (Carnes et al., 2003; Chernoff et al., 1994; Liu and Liebman, 1996; Loenarz et al., 2014; Serio and Lindquist, 1999; Singleton et al., 2014; Velichutina et al., 2000). Another important determinant of readthrough efficiency may be the relative position of the stop codon within the open reading frame (ORF). Experiments in yeast suggested that termination at premature termination codons (PTCs) is slower than that at normal termination codons (NTCs) (Amrani et al., 2004). This apparent difference predicts that readthrough should occur more readily at PTCs than at NTCs, an expectation borne out by results obtained when patients, animals, or cultured cells are treated with the readthrough-promoting drug ataluren (Hirawat et al., 2007; Welch et al., 2007), as well as by recent studies of non-canonical genetic codes in ciliates (Heaphy et al., 2016; Swart et al., 2016; Záhonová et al., 2016).

These functional differences between PTCs and NTCs are consistent with the notion that the position of a PTC within an ORF may influence its termination efficiency and suggest that PTCs closest to the 3′ end of an ORF, i.e., those most likely to have NTC-like contexts, may be the most likely to have high efficiencies of termination, whereas those more 5′ proximal are likely to have reduced termination efficiencies and higher extents of readthrough. Here, we have investigated the role of PTC
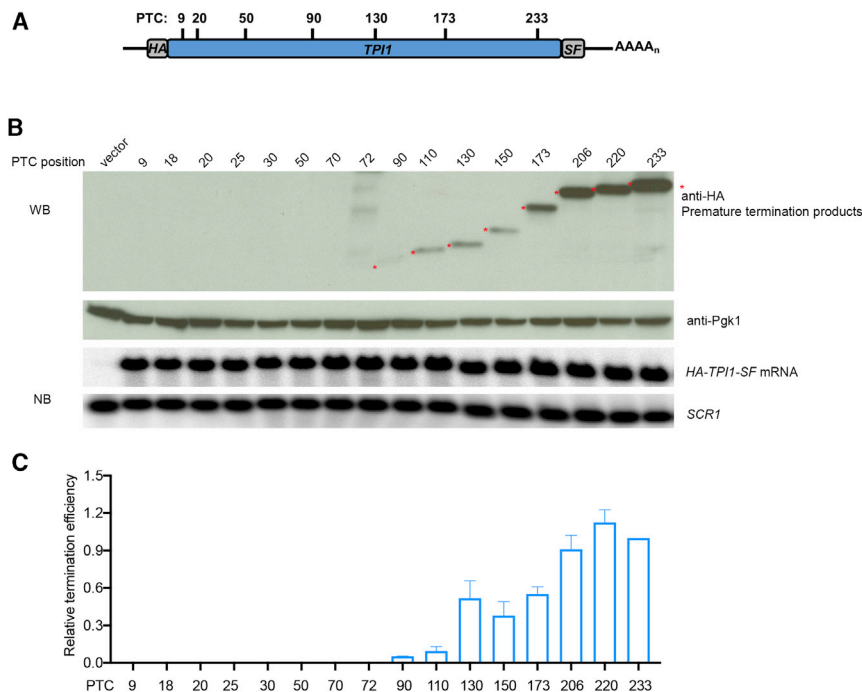
Figure 1. PTC Termination Efficiency Increases across the *TPI1* ORF

(A) *TPI1-PTC* readthrough reporters. Schematic of a subset of the *HA-TPI1-SF* PTC constructs used to analyze translation termination efficiency. HA, S, and F represent HA, StrepII, and FLAG epitope tags, respectively.

(B) Western and northern analyses of prematurely terminated polypeptides and mRNAs expressed from *TPI1-PTC* alleles. Yeast *upf1Δ* cells expressing each of the *TPI1-PTC* alleles were harvested, lysed, and analyzed by western blotting (WB). Anti-HA antibodies detected premature termination products (asterisks), and anti-Pgk1 antibodies detected the Pgk1 control protein. Northern blotting (NB) and phosphorimaging were used to measure the levels of *TPI1-PTC* mRNA and *SCR1* RNA in each sample.

(C) Relative termination efficiency at each *TPI1* PTC. Densitometry was used to quantitate the western blots and the northern blots in (B). Relative termination efficiency was calculated as the relative truncated Tpi1 protein level (anti-HA divided by Pgk1 control) normalized to the relative *TPI1-PTC* mRNA level (mRNA divided by *SCR1* RNA). The efficiency of *TPI1-PTC233* was set as 1. The results shown are the average of three independent experiments ± SEM.

position within an ORF in the regulation of termination and read-through in yeast. We constructed PTCs at multiple positions of the *TPI1*, *LUC*, and *PGK1* ORFs; expressed these alleles in yeast cells inactive for the nonsense-mediated mRNA decay (NMD) pathway; and assessed termination efficiencies and/or read-through at each ORF position by quantitating the premature termination products and/or full-length protein expressed from each PTC allele. Our results revealed a position-dependent effect for termination and readthrough efficiencies and suggested that nonsense codon proximity to the mRNA 3′ end was an important determinant of termination efficiency. Consistent with results of earlier studies implicating a role for poly(A)-binding protein in the regulation of translation termination (Ivanov et al., 2016), we find that deletion of the yeast *PAB1* gene markedly reduces premature termination efficiency, thus yielding substantial enhancement of PTC readthrough.

RESULTS

Efficiency of Premature Termination Increases across the *TPI1* ORF

We constructed a set of reporters in which PTCs were positioned from codons 9 to 233 of the *TPI1* ORF. Each allele has a stop codon at its designated position, a 3×-hemagglutinin (HA) tag at the ORF N terminus, and a StrepII-FLAG (SF) tag at the ORF C terminus. All *TPI1* cassettes were cloned into the pRS315 yeast centromere vector, flanked by the promoter, 5′ UTR, and 3′ UTR of the *TPI1* gene. We used a weak terminator and weak context (UGA CAA) (Bonetti et al., 1995) for each PTC reporter while including a strong terminator (UAA) at the NTC.

Upf1 is a key regulator of NMD, and deletion of its gene in yeast not only stabilizes nonsense-containing mRNAs but also

enhances nonsense codon readthrough and inhibits the degradation of prematurely terminated polypeptides (He and Jacobson, 2015; Johansson and Jacobson, 2010; Kuroha et al., 2009; Leeds et al., 1991). Hence, to stabilize premature termination products, augment detection of readthrough, and minimize variability in mRNA levels, we performed all experiments in *upf1Δ* cells. Each *TPI1-PTC* reporter and an empty vector was transformed into *upf1Δ* cells, and the resulting strains were grown, harvested, and analyzed in parallel. Premature termination products, identified and quantitated by western blotting (WB) with anti-HA antibodies, could not be detected when a PTC was proximal to the *TPI1* ORF N terminus (i.e., PTC9 to PTC72), but their levels increased progressively as PTC positions approached the C terminus of the *TPI1* ORF (see PTC90 to PTC233, anti-HA, Figure 1B; Table S3, sheet 1).

Relative termination efficiencies at *TPI1* PTCs (Figure 1C) were determined by normalizing anti-HA WB results to the level of an internal control protein (Pgk1) in the same samples (Figure 1B, bottom WB panel) and to the level of the corresponding *TPI1-PTC* mRNA in each sample (determined by northern blotting [NB] and normalized to a control RNA, *SCR1*; Figure 1B, NB panels; Table S3, sheet 1). The relative termination efficiencies of *TPI1* PTCs showed a position effect in which termination efficiency was too low to measure within early parts of the *TPI1* ORF but increased progressively from PTC90 to the end of the *TPI1* ORF (Figure 1C).

PTC Readthrough Efficiency Decreases across the *LUC* ORF

Our observation that the efficiency of premature termination appears to improve at least 15-fold as the position of a PTC approaches the 3′ end of the *TPI1* ORF (Figure 1) suggested that

the readthrough efficiency of PTCs should manifest the inverse, i.e., a systematic decrease across an ORF. Accordingly, we constructed a set of reporters with PTCs positioned at six locations within the firefly luciferase (*LUC*) ORF (Figure 2A). These *LUC-PTC* reporters have the same regulatory elements, epitope tags, and termination codon usage as the *TPI1-PTC* reporters. *LUC-PTC* reporters, an NTC reporter (lacking any PTC in the coding region), and a vector control were transformed into *upf1Δ* cells; and the resulting strains were analyzed as in Figure 1. Readthrough efficacy was assessed by WB with anti-FLAG antibodies to monitor the accumulation of full-length luciferase protein (Figure 2B, top panel). Relative readthrough efficiencies (Figure 2D; Table S3, sheet 2) were determined by normalizing the anti-FLAG WB results to the level of a control protein (Pgk1) (Figure 2B, bottom panel) and to the level of *LUC* mRNA in each sample (determined by NB and also normalized to a control RNA, *SCR1*; Figure 2C). This experiment showed that the extent of readthrough was highest when a PTC was proximal to the N terminus of the *LUC* ORF (PTC20 and PTC41 showed ~2% of Luc-wt levels) and diminished progressively as the PTC positions approached the C terminus of the ORF (Figure 2B, top panel). After quantitation, the relative readthrough efficiencies of PTCs showed a clear position effect in which readthrough efficiency decreased across the *LUC* ORF (Figure 2D), i.e., readthrough efficiency at each PTC was inversely correlated with its distance to the ORF 3′ end. These variations in readthrough efficiency were unlikely to be due to differences in the stability of the respective full-length readthrough proteins (Kuroha et al., 2009) because treating cells with the proteasome inhibitor MG132 did not alter the relative recovery of readthrough proteins (Figures S2A and S2B).

In parallel with our assays for full-length readthrough proteins, we also used WB with anti-HA antibodies to detect prematurely terminated *LUC* polypeptides. As was seen for early *TPI1* PTC alleles (Figure 1), premature termination products could not be detected from *LUC* PTC20 and PTC41 but were readily detected from PTC160, PTC386, PTC460, and PTC520 (Figure 2B, middle panel, and Figure S2A, middle panel; see red asterisks). Corrected for the Pgk1 control protein and *LUC* mRNA levels, the recovery of prematurely terminated polypeptides showed a general upward trend from PTC160 to PTC460, a result supported by our observation of decreased readthrough across the same region of the *LUC* ORF (Figures 2, S2A, and S2B) and with similar measurements of premature termination efficiencies in *TPI1-PTC* reporters (Figure 1).

Our inability to detect any premature termination products from early PTCs in the *TPI1* and *LUC* mRNAs was not likely to be due to their susceptibility to proteasomal degradation (Figures S2A and S2B), their failure to be recovered by WB, or to some previously unknown mechanism that degrades short nascent polypeptides while they are still associated with tRNA. The latter two conclusions follow from the WB detection of (1) a synthetic polypeptide containing the 3×-HA epitope and the first 19 amino acids of luciferase (i.e., the polypeptide that would be generated by premature termination at PTC20) (Figure S2C); and (2) peptidyl-tRNAs from *LUC-PTC20* and *LUC-PTC41* (Figures S2D and S2E).

The Ratios of Full-Length Readthrough Product to the Corresponding Prematurely Terminated Product at Each PTC Vary as a Function of ORF Position

As an independent approach for assessing changes in readthrough efficiency across an ORF, we measured changes in the ratio of prematurely terminated polypeptide relative to the accumulation of full-length readthrough protein, and both were simultaneously detected with the same antibody. The anti-HA western blot of Figure 2B used to identify premature termination products also detected full-length Luc protein derived from PTC readthrough (middle panel, top band, see arrow). As shown in Figure S1B, the ratio of recoverable premature termination products to the full-length readthrough protein increased substantially from PTC160 to PTC520, a result consistent with a progressive improvement in termination efficiency as the ribosome approached the NTC. Variable recoveries of the full-length readthrough product precluded a similar analysis for *TPI1*, but we were able to determine the ratio of prematurely terminated products to full-length readthrough protein with the *PGK1* gene. We constructed a set of *PGK1* reporters flanked by the promoter, 5′ UTR, and 3′ UTR of the *PGK1* gene and with PTCs positioned at codons 37, 84, 219, and 309 (Figure 3A). Each *PGK1-PTC* reporter had the same weak terminator, epitope tags, and plasmid backbone as the *TPI1-PTC* reporters. *PGK1-PTC* reporters and the control vector were transformed into *upf1Δ* cells that were analyzed by the same procedures used above for the *TPI1-PTC* and *LUC-PTC* reporters. This experiment showed that the extent of readthrough was highest when a PTC was proximal to the N terminus of the *PGK1* ORF and diminished progressively as the PTC positions approached the C terminus of the ORF (Figure 3B, top bands in anti-HA blot), whereas the extent of termination showed the opposite trend (Figure 3B, bottom bands in anti-HA blot). After being normalized to *PGK1-PTC* mRNA levels (Figure 3C), the relative readthrough and termination efficiencies of PTCs showed clear position effects in which readthrough efficiency decreased and termination efficiency increased across the *PGK1* ORF (Figures 3D and 3E), consistent with the *LUC-PTC* and *TPI1-PTC* results. Importantly, the ratio of premature termination product to readthrough product of each allele also showed an upward trend across the *PGK1* ORF, indicating a progressive improvement of termination efficiency as PTCs approached the ORF C terminus (Figure 3F).

3′ UTR Length Regulates the Efficiency of PTC Readthrough

Earlier studies suggested that interactions between mRNA-associated poly(A)-binding protein (Pab1 in yeast) and eRF3 enhance translation termination efficiency (Amrani et al., 2004; Heaphy et al., 2016; Ivanov et al., 2016; Roque et al., 2015; Swart et al., 2016; Záhonová et al., 2016). To test whether the progressive changes in termination and readthrough efficiencies we observed with *TPI1*, *LUC*, and *PGK1* PTC mutations reflected changes in PTC proximity to Pab1 (or any other 3′ UTR-localized regulatory factor), we began with the *LUC* reporter manifesting the least efficient readthrough (*LUC-PTC520*) and constructed a series of *LUC-PTC520* alleles having 3′ UTR lengths ranging

A

B

C

D
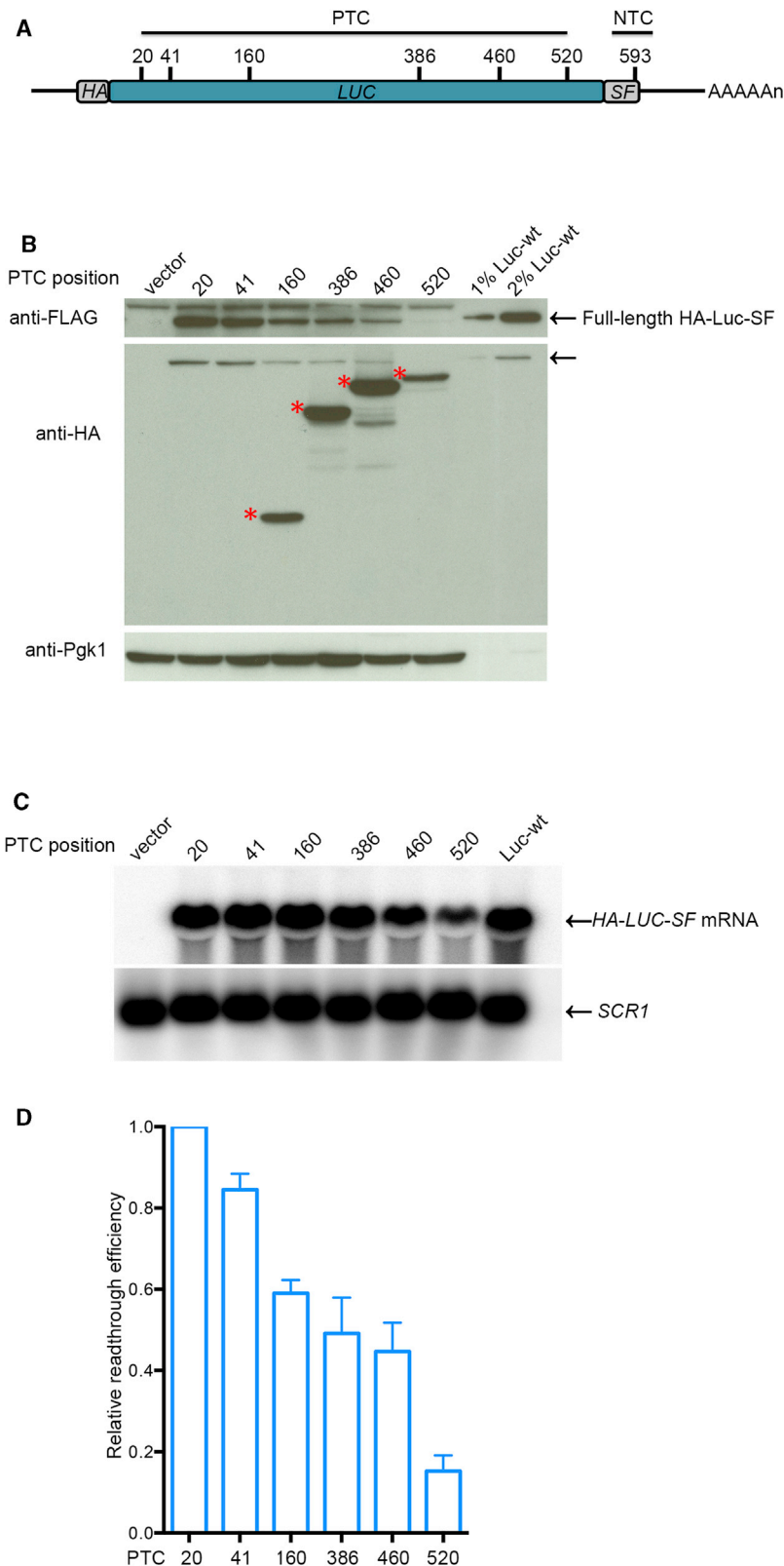
Figure 2. PTC Readthrough Efficiency Decreases across the *LUC* ORF

(A) *LUC-PTC* readthrough reporters. Schematic of the positions of PTCs and the NTC in *HA-LUC-SF* constructs. HA, S, and F represent HA, StrepII, and FLAG epitope tags, respectively.

(B) Western analysis of full-length readthrough proteins and prematurely terminated polypeptides expressed from *LUC-PTC* alleles. Yeast *upf1Δ* cells expressing a *LUC-PTC* allele, a vector control, or a WT *LUC* allele were harvested, lysed, and analyzed by WB by using anti-FLAG antibodies to detect full-length readthrough products, anti-HA antibodies to detect premature termination products, and anti-Pgk1 antibodies to detect the Pgk1 control protein. The arrows (top and middle panels) indicate full-length readthrough protein, and the asterisks (middle panel) indicate premature termination products. Figure S1A shows the complete blot used for the top panel.

(C) Northern analyses of *LUC* mRNA levels in cells expressing PTC alleles. NB and phosphorimaging were used to measure the level of *LUC* mRNA and *SCR1* RNA in each sample.

(D) Relative readthrough efficiency at each of the six *LUC* PTCs. Densitometry was used to quantitate the blots of (B) and (C). Relative readthrough efficiency of each *LUC-PTC* allele was calculated as the ratio of full-length Luc protein level (anti-FLAG) normalized to Pgk1 level divided by *LUC* mRNA level normalized to the level of *SCR1* RNA. The efficiency of *LUC-PTC20* was set as 1. The results shown are the average of three independent experiments ± SEM. 1% and 2% Luc-wt are aliquots of extracts from cells expressing a wild-type *LUC* allele that were 1/100th and 1/50th the volume of samples from cells expressing PTC alleles.
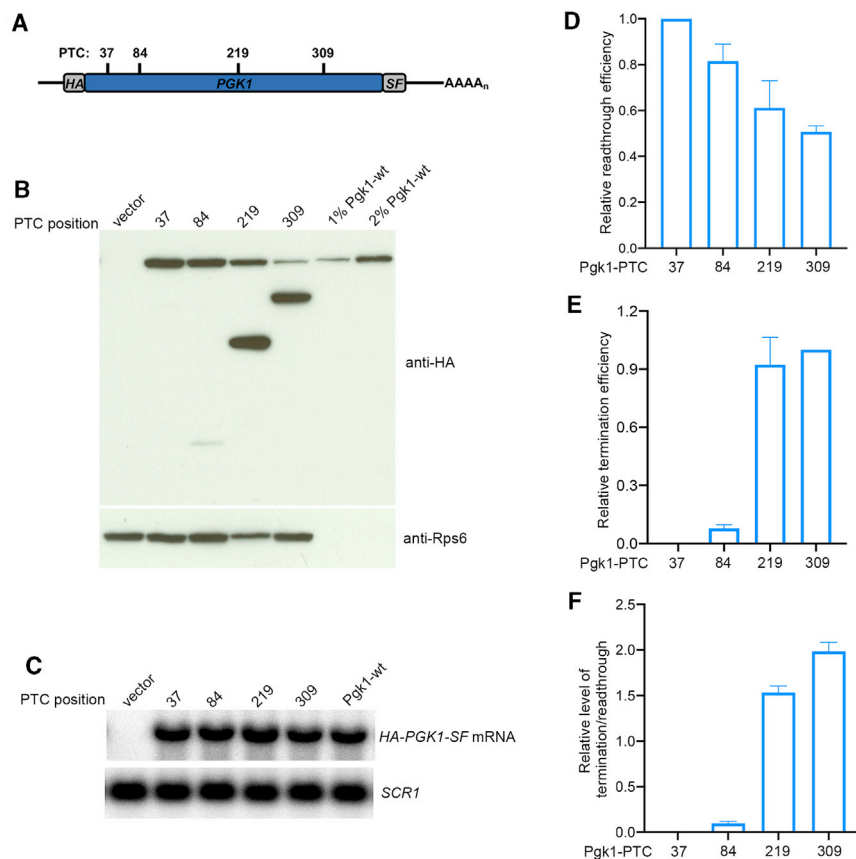
Figure 3. PTC Position Effect on Translation Termination and Readthrough Efficiencies across the *PGK1* ORF

(A) *PGK1-PTC* readthrough reporters. Schematic of PTCs within individual *HA-PGK1-SF* constructs. HA, S, and F represent HA, StrepII, and FLAG epitope tags, respectively.

(B) Western analysis of full-length readthrough proteins and prematurely terminated polypeptides expressed from *PGK1-PTC* alleles. Yeast *upf1Δ* cells expressing a *PGK1-PTC* allele, a vector control, or a wild-type *PGK1* allele were harvested, lysed, and analyzed by WB by using anti-HA antibodies to detect both readthrough and premature termination products and by using anti-Rps6 antibodies to detect the Rps6 control protein.

(C) NB analyses of *PGK1-PTC* mRNA levels in cells expressing different PTC alleles. NB and phosphorimaging were used to measure the level of *PGK1-PTC* mRNA and *SCR1* RNA in each sample.

(D) Relative readthrough efficiency at each of the four *PGK1* PTCs. Densitometry was used to quantitate the blots of (B) and (C). Relative readthrough efficiency of each *PGK1-PTC* allele was calculated as the ratio of full-length Pgk1 protein level (anti-HA, top band) normalized to Rps6 level divided by *PGK1-PTC* mRNA level normalized to the level of *SCR1* RNA. The efficiency of *PGK1-PTC37* was set as 1. The results shown are the average of three independent experiments ± SEM. 1% and 2% Pgk1-wt are aliquots of extracts from cells expressing a wild-type *PGK1* allele that were 1/100th and 1/50th the volume of samples from cells expressing PTC alleles.

(E) Relative termination efficiency at each of the four *PGK1* PTCs. Densitometry was used to quantitate the blots of (B) and (C). Relative termination efficiency of each *PGK1-PTC* allele was calculated as the ratio of truncated Pgk1 protein level (anti-HA, bottom band) normalized to Rps6 level divided by *PGK1-PTC* mRNA level normalized to the level of *SCR1* RNA. The efficiency of *PGK1-PTC309* was set as 1. The results shown are the average of three independent determinations ± SEM.

(F) Ratio of termination to readthrough efficiency at each of the *PGK1* PTCs. Relative termination efficiency at each PTC was calculated as the ratio of termination efficiency in (E) divided by readthrough efficiency in (D).

from 60 to 600 nucleotides (nt) (Figure 4A). Quantitation of the expression of these alleles in *upf1Δ* cells showed that the relative readthrough efficiencies increased progressively with 3′ UTR length (Figures 4B and 4C), i.e., the results indicate that the length of the 3′ UTR associated with the *LUC* mRNA plays an important *cis*-acting role in regulating translational readthrough of PTCs in yeast.

Poly(A)-Binding Protein Restricts PTC Readthrough and Controls the PTC Position Effect

In light of the correlation between 3′ UTR length and PTC readthrough seen in Figure 4 and earlier studies addressing Pab1:eRF3 interactions (Roque et al., 2015), we sought to directly test whether the observed readthrough phenotypes reflected PTC proximity to the mRNA-associated Pab1 protein. *PAB1* is an essential gene in yeast (Sachs et al., 1987), but its absence can be studied in several suppressor mutants. Pbp1 was identified as a Pab1-interacting protein, and *pbp1Δ* cells suppress a *pab1Δ* allele without having significant effects on mRNA translation or decay (Kato et al., 2019; Mangus et al., 1998; Yang et al., 2019). Accordingly, we generated *pab1Δ pbp1Δ upf1Δ* yeast

cells and transformed them with the *pRS316-LUC-PTC* reporters and control plasmids equivalent to those analyzed in the experiments of Figure 2. As additional controls, each reporter was also transformed into *pbp1Δ upf1Δ* cells. Readthrough efficiencies were determined in *upf1Δ*, *pbp1Δ upf1Δ*, and *pab1Δ pbp1Δ upf1Δ* cells; and the results of these analyses are shown in Figure 5. Consistent with previous conclusions about the modest impact of the *pbp1Δ* allele on mRNA translation and decay, we found the relative readthrough efficiencies of *LUC-PTC* reporters in *pbp1Δ upf1Δ* cells to be quite similar to those seen in *upf1Δ* cells (Figure 5C). However, in *pab1Δ pbp1Δ upf1Δ* cells, the relative readthrough efficiencies of all *LUC-PTC* reporters were much higher than those in *upf1Δ* or *pbp1Δ upf1Δ* cells (Figure 5C), with readthrough efficiencies of *LUC-PTCs* in *pab1Δ pbp1Δ upf1Δ* cells approximately 2- to 8-fold higher than those observed in the two other strains. Readthrough efficiencies across the *LUC* ORF in *upf1Δ* cells continuously decreased as the ribosome progressed from 5′ to 3′, whereas in *pab1Δ pbp1Δ upf1Δ* cells, this gradient was absent and was replaced by a "bell-shaped" distribution of readthrough activity across the ORF. Furthermore, in contrast to the increased levels
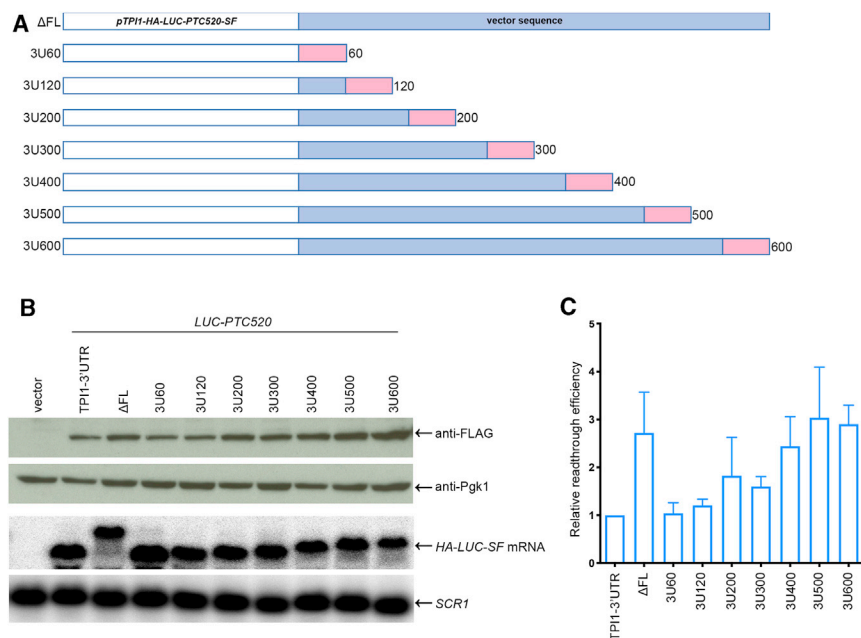
Figure 4. The Efficiency of Readthrough of *LUC-PTC520* mRNA Varies Directly with the Length of Its Associated 3′ UTR

(A) Schematic representation of *LUC-PTC520* alleles with defined 3′ UTR lengths. The *GAL7* cleavage/polyadenylation signal (pink rectangles) was inserted at different locations downstream of the *LUC-PTC520* ORF (ΔFL allele, full-length *TPI1* 3′ UTR was deleted) to generate a set of *LUC-PTC520* alleles that were transformed into *upf1Δ* cells for an assessment of *LUC* mRNA and protein expression. mRNAs from this set of alleles have 3′ UTR lengths ranging from 60 to 600 nt. pTPI1, *TPI1* promoter; SF, StrepII-FLAG tag; FL, full-length *TPI1* 3′ region.

(B) Analyses of the mRNAs and readthrough products generated by *LUC-PTC520* alleles with defined 3′ UTR lengths. *LUC-PTC520* alleles harboring 3′ UTRs of 60–600 bp were expressed in *upf1Δ* cells and lysates of the respective cells were analyzed by WB and NB as in Figure 2.

(C) Relative readthrough efficiencies of *LUC-PTC520* alleles with 3′ UTRs of defined lengths. Relative readthrough efficiencies were calculated as in Figure 2D. The results shown are the average of four independent experiments ± SEM. The efficiency of *TPI1*-3′ UTR was set as 1.

of *LUC* readthrough proteins (Figure 5A, top panel), the premature termination products were much lower in *pab1Δ pbp1Δ upf1Δ* cells than in the other two strains (Figure 5A, middle panel), with several premature termination products beyond detection when western blots were exposed for similar times. The presence of prematurely terminated products in *pab1Δ pbp1Δ upf1Δ* cells could be detected if blots were exposed for longer times (Figure S3). Although the termination efficiencies of *LUC-PTCs* in *pab1Δ pbp1Δ upf1Δ* cells could not be compared properly in parallel with those in *upf1Δ* or *pbp1Δ upf1Δ* cells, termination efficiencies in *pbp1Δ upf1Δ* cells could be compared to those in *upf1Δ* cells, and they were found to be 1.5- to 2-fold lower (Figure S4A).

The results of Figure 5 demonstrated that Pab1 enhanced termination and restricted PTC readthrough *in vivo*. In order to assign that function to specific Pab1 domains, we examined the consequences of deleting the C-terminal domain of the protein, the region thought to interact with eRF3 (Roque et al., 2015). This deletion does not impair yeast cell viability (Sachs et al., 1987). We constructed *pab1ΔC upf1Δ* cells, transformed them with *LUC-PTC* and control reporters, and evaluated PTC readthrough efficiency in these cells. Figure S5A (top panel) shows that the yields of full-length proteins from all six *LUC-PTCs* in *pab1ΔC upf1Δ* cells were higher than in *upf1Δ* cells. After correction for protein and mRNA controls (Figures S5A, bottom panel, and S5B), the relative readthrough efficiencies of PTCs in *pab1ΔC upf1Δ* cells were 2- to 4-fold higher than those of the same alleles in *upf1Δ* cells (Figure S5C). Readthrough efficiencies in *pab1ΔC upf1Δ* cells were flat across the first two-thirds of the *LUC* ORF but decreased for the last two alleles. Although premature termination products were detectable in *pab1ΔC upf1Δ* cells, their termination efficiencies were lower than those in *upf1Δ* cells (Figure S4B).

DISCUSSION

PTC Position Effects in the *TPI1*, *LUC*, and *PGK1* ORFs Are Associated with Variations in the Efficiency of Translation Termination

The mechanisms regulating termination efficiency and nonsense codon readthrough remain poorly understood. Here, by using three independent reporter assays as criteria for the extent of termination at a given PTC, we demonstrate that the position of a PTC within an ORF dictates its termination and/or readthrough efficiency. In support of this conclusion, we find that (1) PTCs proximal to the 5′ end of an ORF have higher readthrough efficiencies than PTCs proximal to the 3′ end of the same ORF (Figures 2B, 2D, 3B, 3D, 5A, 5C, S1A, S2A, S2B, S5A, and S5C); (2) premature termination efficiencies largely appear to increase across the same regions (Figures 1B, 1C, 2B, 3B, 3E, 5A, S2A, S3, S4A, S4B, and S5A); and (3) consistent with the respective descending and ascending efficiencies of readthrough and termination efficiency across an ORF, the ratio of termination products to readthrough products increases progressively toward the mRNA NTC (Figures S1B and 3F). Note that values for all the readthrough and termination efficiencies are relative, not absolute percentages.

Premature termination products could not be detected from *TPI1*, *LUC*, and *PGK1* mRNAs with "early" PTCs, a shortcoming that we could not account for by deficiencies in protein stability, gel transfer, or accumulation of the respective peptidyl-tRNAs (Figure S2). The consistency of the phenomenon with three different sets of premature termination products suggests that the detection of short prematurely terminated polypeptides may be limited by the overall expression levels of the respective genes or that they are targeted for degradation by a specific proteolytic pathway that does not use the proteasome. In light of the
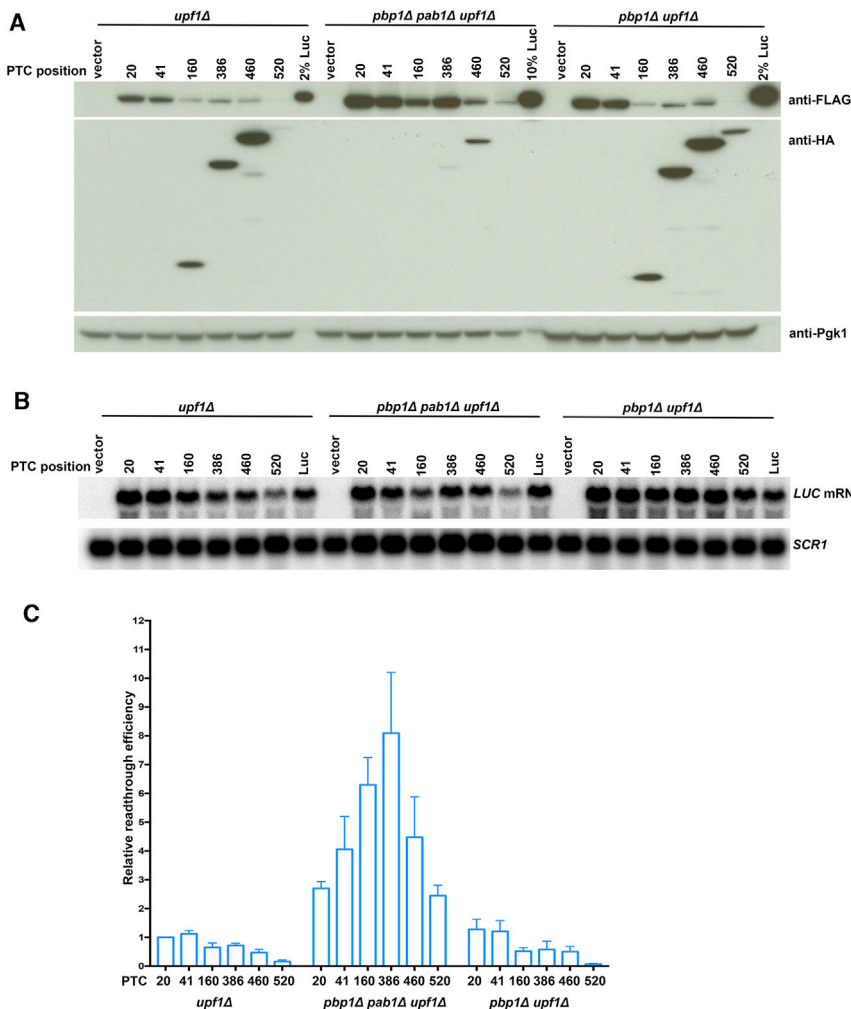
Figure 5. Deletion of *PAB1* Enhances Translational Readthrough and Disrupts PTC Position Effects

(A) Western analyses of *LUC-PTC* reporters expressed in *upf1Δ*, *pab1Δ pbp1Δ upf1Δ*, and *pbp1Δ upf1Δ* cells. Yeast *upf1Δ*, *pab1Δ pbp1Δ upf1Δ*, or *pbp1Δ upf1Δ* cells expressing a *LUC* PTC allele, a vector control, or wild-type *LUC* were harvested, lysed, and analyzed by WB as in Figure 2. 10% Luc is an aliquot of extract from cells expressing a wild-type *LUC* allele that was 1/10th the total protein of samples from cells expressing PTC alleles.

(B) Northern analyses of *LUC-PTC* reporter mRNA expression in *upf1Δ*, *pab1Δ pbp1Δ upf1Δ*, and *pbp1Δ upf1Δ* cells. Yeast cells shown in (A) were analyzed for *LUC* mRNA levels as in Figure 2.

(C) Relative readthrough efficiencies of different *LUC-PTC* reporters in cells with and without Pab1. Relative readthrough efficiencies of the *LUC-PTC* alleles in *upf1Δ*, *pab1Δ pbp1Δ upf1Δ*, and *pbp1Δ upf1Δ* cells were calculated as in Figure 2D. The results shown are the average of three independent experiments ± SEM.

(Swart et al., 2016). As discussed below, the poly(A)-binding protein also appears to be a critical regulator of the PTC position effects in yeast.

Yeast Pab1 Is a Key Determinant of the PTC Position Effect

The multiple experimental approaches described here implicate a role for Pab1 in the regulation of termination efficiency and PTC readthrough. First, we observed a trend toward higher efficiencies of premature translation termination as PTCs approached the 3′ ends of three different ORFs (Figures 1B, 1C, 3B, 3E, 3F, 5A, S1B, S2A, S3, S4A, S4B, and S5A). Second, we observed an inverse correlation between the extent of readthrough at a given PTC and the distance of that PTC from the respective mRNA 3′ end, i.e., the position of the poly(A) tail (Figures 2B, 2D, 3B, 3D, 4B, 4C, 5A, 5C, S1A, S2A, S2B, S5A, and S5C). This was true for PTCs at different ORF positions (e.g., Figures 2 and 3), as well as for *LUC* PTC520 when it was associated with 3′ UTRs of different lengths (Figure 4). Although these results provide only indirect evidence for a Pab1 role in termination regulation, an additional set of experiments provided direct evidence for that role. Figure 5 shows that deletion of the *PAB1* gene leads to large increases in readthrough efficiency at all PTC positions, comparably large reductions in termination efficiency, and loss of the progressive PTC position effects across the *LUC* ORF. Furthermore, the experiments of Figure 5 demonstrate that the *pbp1Δ* mutation required for the maintenance of viability in *pab1Δ* cells does not contribute to these effects.

A role for Pab1 in restricting readthrough is consistent with results of several earlier studies in multiple systems, including those reporting (1) position dependence of the non-canonical

complementary and confirmatory results we obtained from readthrough assays and from the ratio of premature termination products to readthrough products, we do not consider the selective loss of a subset of premature termination products to have weakened the argument for an ORF-wide gradient of termination efficiency.

The position dependence of nonsense codon function observed in our experiments is reminiscent of the non-canonical genetic code use in some species of protozoa, in which all three nonsense codons function as sense codons unless they are located near ORF 3′ ends, where they still serve their usual termination function (Heaphy et al., 2016; Swart et al., 2016; Záhonová et al., 2016). The decoding of UAA, UAG, and UGA in these atypical genetic codes appears to be mediated in part by mutations that lessen the specificity of eRF1 and make it an ineffective competitor with tRNAs capable of nonsense codon recognition (Swart et al., 2016). The enhanced specificity of the same eRF1 molecules when ribosomes are translating near the end of ORFs is postulated to arise from proximity to 3′-end-associated poly(A)-binding protein and its stimulatory effects on eRF3, which is the release factor that normally augments eRF1 function

genetic codes in ciliates (see above) (Heaphy et al., 2016; Swart et al., 2016; Záhonová et al., 2016); (2) interactions between eRF3 and PABP from mammalian, *Xenopus*, and yeast cells, and identification of specific interacting domains in the respective proteins (Cosson et al., 2002a, 2002b; Hoshino et al., 1999; Hosoda et al., 2003; Jerbi et al., 2016; Kononenko et al., 2010; Roque et al., 2015; Uchida et al., 2002); and (3) direct stimulation of peptidyl-tRNA hydrolysis dependent on a eRF3:PABP interaction in a reconstituted cell-free system (Ivanov et al., 2016). However, our results differ from those of Roque et al. (2015) who found that readthrough efficiency in a dual-luciferase assay in yeast decreased when the Pab1:eRF3 interaction was interrupted. A significant difference between our study and that of Roque et al. (2015) that may account for this difference was their inclusion of suppressor tRNA in the strains being tested, i.e., their assays focused on the strong but artificial readthrough signals generated by a cognate suppressor tRNA, whereas ours addressed the competition between eRF1 and nc-tRNAs that is typical of conventional PTC readthrough (Roy et al., 2015, 2016).

The Inefficiency of Premature Termination May Define Susceptibility to NMD

Our results have important implications for NMD. In addition to providing *in vivo* substantiation of our earlier *in vitro* studies that indicated fundamental mechanistic differences between normal and premature translation termination (Amrani et al., 2004), our results suggest further insights. Earlier work on NMD in yeast showed that PTCs within the first half to two-thirds of an ORF triggered NMD, whereas those in the latter part of an ORF had little to no mRNA destabilizing effects (Hagan et al., 1995; Hennigan and Jacobson, 1996, 1997; Peltz et al., 1993, 1994; Peltz and Jacobson, 1993). We observed a similar phenomenon when the relative abundance of *LUC* mRNAs harboring the six PTCs studied here was analyzed in wild-type (WT) cells (Figure S1C). It has been shown that such PTC position effects on NMD could be mimicked and manipulated by shortening or lengthening mRNA 3′ UTRs (Amrani et al., 2004; Kebaara and Atkin, 2009; Muhlrad and Parker, 1999) and that NMD can be antagonized by tethering Pab1 or eRF3 proximal to a PTC (Amrani et al., 2004). These results, and toeprinting experiments indicating that termination at PTCs had a much longer dwell time than that at NTCs (Amrani et al., 2004), led to the formulation of the *faux*-UTR model for NMD that postulated that the inefficient termination occurring at PTCs distant from 3′-end-localized Pab1 allowed for mRNA binding of the Upf factors that trigger NMD (Amrani et al., 2004, 2006a, 2006b; Amrani and Jacobson, 2006). Although the experiments of this study were carried out in NMD-deficient cells, the results reported here and the earlier data supporting the *faux*-UTR model strongly suggest that a threshold level of termination inefficiency is a trigger for NMD, possibly because the ribosome is transiently in a state that allows association of the Upf factors (He and Jacobson, 2015).

STAR★METHODS

Detailed methods are provided in the online version of this paper and include the following:

- KEY RESOURCES TABLE
- RESOURCE AVAILABILITY
  - Lead Contact
  - Materials Availability
  - Data and Code Availability
- EXPERIMENTAL MODEL AND SUBJECT DETAILS
- METHOD DETAILS
  - Yeast strains and plasmid constructs
  - Cell growth and western analysis
  - Detection of peptidyl-tRNA
  - RNA preparation and northern analysis
- QUANTIFICATION AND STATISTICAL ANALYSIS

AUTHOR CONTRIBUTIONS

C.W., B.R., F.H., and A.J. conceived and designed the experiments; C.W., B.R., and K.Y. carried out the experiments; C.W. and A.J. wrote the paper with input from all authors; and A.J. obtained funding for the study.

REFERENCES

Alkalaeva, E.Z., Pisarev, A.V., Frolova, L.Y., Kisselev, L.L., and Pestova, T.V. (2006). In vitro reconstitution of eukaryotic translation reveals cooperativity between release factors eRF1 and eRF3. Cell *125*, 1125–1136.

Amrani, N., and Jacobson, A. (2006). All termination events are not equal: premature termination is aberrant and triggers NMD. In Nonsense-mediated mRNA decay, L.E. Maquat, ed. (Landes Bioscience), pp. 15–25.

Amrani, N., Ganesan, R., Kervestin, S., Mangus, D.A., Ghosh, S., and Jacobson, A. (2004). A faux 3′-UTR promotes aberrant termination and triggers nonsense-mediated mRNA decay. Nature *432*, 112–118.

Amrani, N., Dong, S., He, F., Ganesan, R., Ghosh, S., Kervestin, S., Li, C., Mangus, D.A., Spatrick, P., and Jacobson, A. (2006a). Aberrant termination triggers nonsense-mediated mRNA decay. Biochem. Soc. Trans. *34*, 39–42.

Amrani, N., Sachs, M.S., and Jacobson, A. (2006b). Early nonsense: mRNA decay solves a translational problem. Nat. Rev. Mol. Cell Biol. *7*, 415–425.

Anzalone, A.V., Zairis, S., Lin, A.J., Rabadan, R., and Cornish, V.W. (2019). Interrogation of Eukaryotic Stop Codon Readthrough Signals by in Vitro RNA Selection. Biochemistry *58*, 1167–1178.

Bonetti, B., Fu, L., Moon, J., and Bedwell, D.M. (1995). The efficiency of translation termination is determined by a synergistic interplay between upstream

and downstream sequences in *Saccharomyces cerevisiae*. J. Mol. Biol. *251*, 334–345.

Brenner, S., Stretton, A.O., and Kaplan, S. (1965). Genetic code: the 'nonsense' triplets for chain termination and their suppression. Nature *206*, 994–998.

Brown, A., Shao, S., Murray, J., Hegde, R.S., and Ramakrishnan, V. (2015). Structural basis for stop codon recognition in eukaryotes. Nature *524*, 493–496.

Bucheli, M.E., He, X., Kaplan, C.D., Moore, C.L., and Buratowski, S. (2007). Polyadenylation site choice in yeast is affected by competition between Npl3 and polyadenylation factor CFI. RNA *13*, 1756–1764.

Carnes, J., Jacobson, M., Leinwand, L., and Yarus, M. (2003). Stop codon suppression via inhibition of eRF1 expression. RNA *9*, 648–653.

Chernoff, Y.O., Vincent, A., and Liebman, S.W. (1994). Mutations in eukaryotic 18S ribosomal RNA affect translational fidelity and resistance to aminoglycoside antibiotics. EMBO J. *13*, 906–913.

Cosson, B., Berkova, N., Couturier, A., Chabelskaya, S., Philippe, M., and Zhouravleva, G. (2002a). Poly(A)-binding protein and eRF3 are associated *in vivo* in human and *Xenopus* cells. Biol. Cell *94*, 205–216.

Cosson, B., Couturier, A., Chabelskaya, S., Kiktev, D., Inge-Vechtomov, S., Philippe, M., and Zhouravleva, G. (2002b). Poly(A)-binding protein acts in translation termination via eukaryotic release factor 3 interaction and does not influence [PSI(+)] propagation. Mol. Cell. Biol. *22*, 3301–3315.

Cridge, A.G., Crowe-McAuliffe, C., Mathew, S.F., and Tate, W.P. (2018). Eukaryotic translational termination efficiency is influenced by the 3′ nucleotides within the ribosomal mRNA channel. Nucleic Acids Res. *46*, 1927–1944.

Hagan, K.W., Ruiz-Echevarria, M.J., Quan, Y., and Peltz, S.W. (1995). Characterization of *cis*-acting sequences and decay intermediates involved in nonsense-mediated mRNA turnover. Mol. Cell. Biol. *15*, 809–823.

Harrell, L., Melcher, U., and Atkins, J.F. (2002). Predominance of six different hexanucleotide recoding signals 3′ of read-through stop codons. Nucleic Acids Res. *30*, 2011–2017.

He, F., and Jacobson, A. (1995). Identification of a novel component of the nonsense-mediated mRNA decay pathway by use of an interacting protein screen. Genes Dev. *9*, 437–454.

He, F., and Jacobson, A. (2015). Nonsense-mediated mRNA decay: Degradation of defective transcripts is only part of the story. Annu. Rev. Genet. *49*, 339–366.

He, F., Brown, A.H., and Jacobson, A. (1997). Upf1p, Nmd2p, and Upf3p are interacting components of the yeast nonsense-mediated mRNA decay pathway. Mol. Cell. Biol. *17*, 1580–1594.

Heaphy, S.M., Mariotti, M., Gladyshev, V.N., Atkins, J.F., and Baranov, P.V. (2016). Novel Ciliate Genetic Code Variants Including the Reassignment of All Three Stop Codons to Sense Codons in Condylostoma magnum. Mol. Biol. Evol. *33*, 2885–2889.

Hennigan, A.N., and Jacobson, A. (1996). Functional mapping of the translation-dependent instability element of yeast MATalpha1 mRNA. Mol. Cell. Biol. *16*, 3833–3843.

Hennigan, A.N., and Jacobson, A. (1997). A genetic approach to mapping coding region determinants of mRNA stability in yeast. In mRNA Formation and Function, J.D. Richter, ed. (Academic Press), pp. 149–161.

Herrick, D., Parker, R., and Jacobson, A. (1990). Identification and comparison of stable and unstable mRNAs in Saccharomyces cerevisiae. Mol. Cell. Biol. *10*, 2269–2284.

Hirawat, S., Welch, E.M., Elfring, G.L., Northcutt, V.J., Paushkin, S., Hwang, S., Leonard, E.M., Almstead, N.G., Ju, W., Peltz, S.W., and Miller, L.L. (2007). Safety, tolerability, and pharmacokinetics of PTC124, a nonaminoglycoside nonsense mutation suppressor, following single- and multiple-dose administration to healthy male and female adult volunteers. J. Clin. Pharmacol. *47*, 430–444.

Hoshino, S., Hosoda, N., Araki, Y., Kobayashi, T., Uchida, N., Funakoshi, Y., and Katada, T. (1999). Novel function of the eukaryotic polypeptide-chain releasing factor 3 (eRF3/GSPT) in the mRNA degradation pathway. Biochemistry (Mosc.) *64*, 1367–1372.

Hosoda, N., Kobayashi, T., Uchida, N., Funakoshi, Y., Kikuchi, Y., Hoshino, S., and Katada, T. (2003). Translation termination factor eRF3 mediates mRNA decay through the regulation of deadenylation. J. Biol. Chem. *278*, 38287–38291.

Howard, M.T., Shirts, B.H., Petros, L.M., Flanigan, K.M., Gesteland, R.F., and Atkins, J.F. (2000). Sequence specificity of aminoglycoside-induced stop condon readthrough: potential implications for treatment of Duchenne muscular dystrophy. Ann. Neurol. *48*, 164–169.

Ivanov, A., Mikhailova, T., Eliseev, B., Yeramala, L., Sokolova, E., Susorov, D., Shuvalov, A., Schaffitzel, C., and Alkalaeva, E. (2016). PABP enhances release factor recruitment and stop codon recognition during translation termination. Nucleic Acids Res. *44*, 7766–7776.

Jerbi, S., Jolles, B., Bouceba, T., and Jean-Jean, O. (2016). Studies on human eRF3-PABP interaction reveal the influence of eRF3a N-terminal glycin repeat on eRF3-PABP binding affinity and the lower affinity of eRF3a 12-GGC allele involved in cancer susceptibility. RNA Biol. *13*, 306–315.

Johansson, M.J., and Jacobson, A. (2010). Nonsense-mediated mRNA decay maintains translational fidelity by limiting magnesium uptake. Genes Dev. *24*, 1491–1495.

Kato, M., Yang, Y.S., Sutter, B.M., Wang, Y., McKnight, S.L., and Tu, B.P. (2019). Redox State Controls Phase Separation of the Yeast Ataxin-2 Protein via Reversible Oxidation of Its Methionine-Rich Low-Complexity Domain. Cell *177*, 711–721.e718.

Kebaara, B.W., and Atkin, A.L. (2009). Long 3′-UTRs target wild-type mRNAs for nonsense-mediated mRNA decay in Saccharomyces cerevisiae. Nucleic Acids Res. *37*, 2771–2778.

Keeling, K.M., Xue, X., Gunn, G., and Bedwell, D.M. (2014). Therapeutics Based on Stop Codon Readthrough. Annu. Rev. Genomics Hum. Genet. *15*, 371–394.

Kessler, S.H., and Sachs, A.B. (1998). RNA recognition motif 2 of yeast Pab1p is required for its functional interaction with eukaryotic translation initiation factor 4G. Mol. Cell. Biol. *18*, 51–57.

Kononenko, A.V., Mitkevich, V.A., Atkinson, G.C., Tenson, T., Dubovaya, V.I., Frolova, L.Y., Makarov, A.A., and Hauryliuk, V. (2010). GTP-dependent structural rearrangement of the eRF1:eRF3 complex and eRF3 sequence motifs essential for PABP binding. Nucleic Acids Res. *38*, 548–558.

Kuroha, K., Tatematsu, T., and Inada, T. (2009). Upf1 stimulates degradation of the product derived from aberrant messenger RNA containing a specific nonsense mutation by the proteasome. EMBO Rep. *10*, 1265–1271.

Leeds, P., Peltz, S.W., Jacobson, A., and Culbertson, M.R. (1991). The product of the yeast *UPF1* gene is required for rapid turnover of mRNAs containing a premature translational termination codon. Genes Dev. *5*, 2303–2314.

Liu, R., and Liebman, S.W. (1996). A translational fidelity mutation in the universally conserved sarcin/ricin domain of 25S yeast ribosomal RNA. RNA *2*, 254–263.

Loenarz, C., Sekirnik, R., Thalhammer, A., Ge, W., Spivakovsky, E., Mackeen, M.M., McDonough, M.A., Cockman, M.E., Kessler, B.M., Ratcliffe, P.J., et al. (2014). Hydroxylation of the eukaryotic ribosomal decoding center affects translational accuracy. Proc. Natl. Acad. Sci. USA *111*, 4019–4024.

Longtine, M.S., McKenzie, A., III, Demarini, D.J., Shah, N.G., Wach, A., Brachat, A., Philippsen, P., and Pringle, J.R. (1998). Additional modules for versatile and economical PCR-based gene deletion and modification in Saccharomyces cerevisiae. Yeast *14*, 953–961.

Loughran, G., Chou, M.Y., Ivanov, I.P., Jungreis, I., Kellis, M., Kiran, A.M., Baranov, P.V., and Atkins, J.F. (2014). Evidence of efficient stop codon readthrough in four mammalian genes. Nucleic Acids Res. *42*, 8928–8938.

Mangus, D.A., Amrani, N., and Jacobson, A. (1998). Pbp1p, a factor interacting with *Saccharomyces cerevisiae* poly(A)-binding protein, regulates polyadenylation. Mol. Cell. Biol. *18*, 7383–7396.

Manuvakhova, M., Keeling, K., and Bedwell, D.M. (2000). Aminoglycoside antibiotics mediate context-dependent suppression of termination codons in a mammalian translation system. RNA *6*, 1044–1055.

McCaughan, K.K., Brown, C.M., Dalphin, M.E., Berry, M.J., and Tate, W.P. (1995). Translational termination efficiency in mammals is influenced by the base following the stop codon. Proc. Natl. Acad. Sci. USA *92*, 5431–5435.

Mottagui-Tabar, S., Tuite, M.F., and Isaksson, L.A. (1998). The influence of 5′ codon context on translation termination in Saccharomyces cerevisiae. Eur. J. Biochem. *257*, 249–254.

Muhlrad, D., and Parker, R. (1999). Aberrant mRNAs with extended 3′ UTRs are substrates for rapid degradation by mRNA surveillance. RNA *5*, 1299–1307.

Namy, O., Hatin, I., and Rousset, J.-P. (2001). Impact of the six nucleotides downstream of the stop codon on translation termination. EMBO Rep. *2*, 787–793.

Peltz, S.W., and Jacobson, A. (1993). mRNA Turnover in Saccharomyces cerevisiae. (Academic Press).

Peltz, S.W., Brown, A.H., and Jacobson, A. (1993). mRNA destabilization triggered by premature translational termination depends on at least three *cis*-acting sequence elements and one *trans*-acting factor. Genes Dev. *7*, 1737–1754.

Peltz, S.W., He, F., Welch, E., and Jacobson, A. (1994). Nonsense-mediated mRNA decay in yeast. Prog. Nucleic Acid Res. Mol. Biol. *47*, 271–298.

Peltz, S.W., Morsy, M., Welch, E.M., and Jacobson, A. (2013). Ataluren as an agent for therapeutic nonsense suppression. Annu. Rev. Med. *64*, 407–425.

Roque, S., Cerciat, M., Gaugué, I., Mora, L., Floch, A.G., de Zamaroczy, M., Heurgué-Hamard, V., and Kervestin, S. (2015). Interaction between the poly(A)-binding protein Pab1 and the eukaryotic release factor eRF3 regulates translation termination but not mRNA decay in Saccharomyces cerevisiae. RNA *21*, 124–134.

Roy, B., Leszyk, J.D., Mangus, D.A., and Jacobson, A. (2015). Nonsense suppression by near-cognate tRNAs employs alternative base pairing at codon positions 1 and 3. Proc. Natl. Acad. Sci. USA *112*, 3038–3043.

Roy, B., Friesen, W.J., Tomizawa, Y., Leszyk, J.D., Zhuo, J., Johnson, B., Dakka, J., Trotta, C.R., Xue, X., Mutyam, V., et al. (2016). Ataluren stimulates ribosomal selection of near-cognate tRNAs to promote nonsense suppression. Proc. Natl. Acad. Sci. USA *113*, 12508–12513.

Sachs, A.B., Davis, R.W., and Kornberg, R.D. (1987). A single domain of yeast poly(A)-binding protein is necessary and sufficient for RNA binding and cell viability. Mol. Cell. Biol. *7*, 3268–3276.

Salas-Marco, J., and Bedwell, D.M. (2004). GTP hydrolysis by eRF3 facilitates stop codon decoding during eukaryotic translation termination. Mol. Cell. Biol. *24*, 7769–7778.

Schiestl, R.H., and Gietz, R.D. (1989). High efficiency transformation of intact yeast cells using single stranded nucleic acids as a carrier. Curr. Genet. *16*, 339–346.

Serio, T.R., and Lindquist, S.L. (1999). [PSI+]: an epigenetic modulator of translation termination efficiency. Annu. Rev. Cell Dev. Biol. *15*, 661–703.

Singleton, R., Liu-Yi, P., Formenti, F., Ge, W., Sekirnik, R., Fischer, R., Adam, J., Pollard, P., Wolf, A., Thalhammer, A., et al. (2014). OGFOD1 catalyzes prolyl hydroxylation of RPS23 and is involved in translation control and stress granule formation. Proc. Natl. Acad. Sci. USA *111*, 4031–4036.

Skuzeski, J.M., Nichols, L.M., Gesteland, R.F., and Atkins, J.F. (1991). The signal for a leaky UAG stop codon in several plant viruses includes the two downstream codons. J. Mol. Biol. *218*, 365–373.

Stansfield, I., Jones, K.M., Kushnirov, V.V., Dagkesamanskaya, A.R., Poznya-kovski, A.I., Paushkin, S.V., Nierras, C.R., Cox, B.S., Ter-Avanesyan, M.D., and Tuite, M.F. (1995). The products of the *SUP45* (eRF1) and *SUP35* genes interact to mediate translation termination in *Saccharomyces cerevisiae*. EMBO J. *14*, 4365–4373.

Swart, E.C., Serra, V., Petroni, G., and Nowacki, M. (2016). Genetic Codes with No Dedicated Stop Codon: Context-Dependent Translation Termination. Cell *166*, 691–702.

Tork, S., Hatin, I., Rousset, J.P., and Fabret, C. (2004). The major 5′ determinant in stop codon read-through involves two adjacent adenines. Nucleic Acids Res. *32*, 415–421.

Uchida, N., Hoshino, S., Imataka, H., Sonenberg, N., and Katada, T. (2002). A novel role of the mammalian GSPT/eRF3 associating with poly(A)-binding protein in Cap/Poly(A)-dependent translation. J. Biol. Chem. *277*, 50286–50292.

Velichutina, I.V., Dresios, J., Hong, J.Y., Li, C., Mankin, A., Synetos, D., and Liebman, S.W. (2000). Mutations in helix 27 of the yeast Saccharomyces cerevisiae 18S rRNA affect the function of the decoding center of the ribosome. RNA *6*, 1174–1184.

Welch, E.M., Barton, E.R., Zhuo, J., Tomizawa, Y., Friesen, W.J., Trifillis, P., Paushkin, S., Patel, M., Trotta, C.R., Hwang, S., et al. (2007). PTC124 targets genetic disorders caused by nonsense mutations. Nature *447*, 87–91.

Yang, Y.S., Kato, M., Wu, X., Litsios, A., Sutter, B.M., Wang, Y., Hsu, C.H., Wood, N.E., Lemoff, A., Mirzaei, H., et al. (2019). Yeast Ataxin-2 Forms an Intracellular Condensate Required for the Inhibition of TORC1 Signaling during Respiratory Growth. Cell *177*, 697–710.e617.

Záhonová, K., Kostygov, A.Y., Ševčíková, T., Yurchenko, V., and Eliáš, M. (2016). An Unprecedented Non-canonical Nuclear Genetic Code with All Three Termination Codons Reassigned as Sense Codons. Curr. Biol. *26*, 2364–2369.

Zhouravleva, G., Frolova, L., Le Goff, X., Le Guellec, R., Inge-Vechtomov, S., Kisselev, L., and Philippe, M. (1995). Termination of translation in eukaryotes is governed by two interacting polypeptide chain release factors, eRF1 and eRF3. EMBO J. *14*, 4065–4072.

Cell Reports
Report

STAR★METHODS

KEY RESOURCES TABLE

REAGENT or RESOURCE	SOURCE	IDENTIFIER
Antibodies		
Rabbit polyclonal anti-FLAG	Sigma-Aldrich	Cat#F7425; RRID:AB_439687
Mouse monoclonal anti-OctA-Probe (F-tag-01)	Santa Cruz	Cat#sc-51590; RRID:AB_677316
Mouse monoclonal anti-Pgk1 (22C5D8)	Thermo Fisher	Cat#459250; RRID:AB_2532235
Donkey polyclonal anti-Mouse Secondary	Thermo Fisher	Cat#A24506; RRID:AB_2535975
Donkey anti-Rabbit Secondary	Sigma-Aldrich	Cat#GENA934; RRID:AB_2722659
Mouse monoclonal anti-HA	Sigma-Aldrich	Cat#H3663; RRID:AB_262051
Phospho-S6 Ribosomal Protein (Ser235/236)	Cell Signaling	Cat#4858; RRID:AB_916156
Chemicals, Peptides, and Recombinant Proteins		
Protease inhibitor tablets, EDTA-free	Thermo Fisher	Cat#A32965
dCTP, [α-^{32}P]-6000Ci/mmol	Perkin Elmer	Cat#BLU513Z
MG-132	Sigma-Aldrich	Cat#474790
RNasecure	Thermo Fisher	Cat#7006
Synthetic HA-Luc19: MGYPYDVPDYAGYPYDVPDYAGSYPYD VPDYAMEDAKNIKKGPAPFYPLED	GenScript	This paper
Critical Commercial Assays		
Random Primed DNA Labeling Kit	Sigma-Aldrich	Cat#11004760001
Experimental Models: Organisms/Strains		
S. cerevisiae: *upf1Δ* (HFY871): *MAT**a** ade2-1 his3-11,15 leu2-3,112 trp1-1 ura3-1 can1-100 upf1::HIS3*	Jacobson lab	He et al., 1997
S. cerevisiae: *pab1Δ pbp1Δ upf1Δ*: *MAT**a** ade2-1 his3-11,15 leu2-3,112 trp1-1 ura3-1 can1-100 pab1::HIS3 pbp1::LEU2 upf1::KanMX6*	Jacobson lab	This paper
S. cerevisiae: *pab1ΔC upf1Δ*: *MAT**a** ade2-1 his3-11,15 leu2-3,112 trp1-1 ura3-1 can1-100 pab1ΔC::HIS3 upf1::KanMX6*	Jacobson lab	This paper
S. cerevisiae: *pbp1Δ upf1Δ*: *MAT**a** ade2-1 his3-11,15 leu2-3,112 trp1-1 ura3-1 can1-100 pbp1::LEU2 upf1::KanMX6*	Jacobson lab	This paper
Software and Algorithms		
MultiGauge software	Fujifilm	Science lab 2005

RESOURCE AVAILABILITY

Lead Contact
Further information and requests for resources and reagents should be directed to and will be fulfilled by the Lead Contact, Allan Jacobson (allan.jacobson@umassmed.edu).

Materials Availability
All plasmids and yeast strains generated in this study are available upon request to the lead contact.

Data and Code Availability
This study did not generate any datasets or code.

EXPERIMENTAL MODEL AND SUBJECT DETAILS

Yeast strains used in this study have the W303 background and are listed in the Key Resources Table. Cells were grown in synthetic complete medium lacking the amino acids required to maintain specific plasmids at 30°C.

METHOD DETAILS

Yeast strains and plasmid constructs

The *upf1Δ* strain was described previously (He et al., 1997). Strains combining additional deletions with *upf1Δ*, i.e., *pbp1Δ upf1Δ*, *pab1Δ pbp1Δ upf1Δ*, and *pab1ΔC upf1Δ* were *upf1::KanMX6* derivatives of yDM146, yDM206, and YAS2239 (Kessler and Sachs, 1998; Mangus et al., 1998) and were constructed by PCR-mediated strategies with pFA6a-KanMX6 as the template (Longtine et al., 1998). Fragments amplified by the primer pair upf1-KanMX6-F and upf1-KanMX6-R were transformed into the respective yeast strains by the high-efficiency method (Schiestl and Gietz, 1989). Each genomic DNA deletion was confirmed by PCR analysis with the oligonucleotide pair upf1-SF and upf1-SR.

All of the plasmids and oligonucleotides used in this study are listed in Tables S1 and S2. The pRS315-*TPI1* plasmid was generated by direct PCR cloning of the *TPI1* gene amplified by primer pair TPI1-F(NcoI)/TPI1-R(XhoI). The PCR fragments were digested by NcoI/XhoI and cloned into pRS315-*LUC* digested by NcoI/XhoI. pRS315-*TPI1-PTC* plasmids were generated by overlap PCRs using a common outside primer pair, TPI1-promoter-F (PstI)/TPI13U-R (NotI), and an internal primer pair that introduced PTCs at specific codons: codon 9 (TPI1-PTC9-F/R), codon 18 (TPI1-PTC18-F/R), codon 20 (TPI1-PTC20-F/R), codon 25 (TPI1-PTC25-F/R), codon 30 (TPI1-PTC30-F/R), codon 50 (TPI1-PTC50-F/R), codon 70 (TPI1-PTC70-F/R), codon 72 (TPI1-PTC72-F/R), codon 90 (TPI1-PTC90-F/R), codon 110 (TPI1-PTC110-F/R), codon 130 (TPI1-PTC130-F/R), codon 150 (TPI1-PTC150-F/R), codon 173 (TPI1-PTC173-F/R), codon 206 (TPI1-PTC206-F/R), codon 220 (TPI1-PTC220-F/R), and codon 233 (TPI1-PTC233-F/R). In each case, the final PCR products were digested by PstI/NotI and cloned into pRS315 digested by PstI/NotI.

The plasmid pRS315-*LUC* was generated through subcloning from plasmid YEplac181-HA-LUC-SF (Roy et al., 2015) as follows: First, a PstI-XbaI fragment was isolated from YEplac181-HA-LUC-SF and cloned into the pRS315 vector digested by PstI/XbaI. Then, a *TPI1 3′-UTR* fragment was amplified from YEplac181-HA-LUC-SF by the primer pair TPI13U-F(XbaI)/TPI13U-R(NotI), digested by XbaI/NotI, and ligated into pRS315-*TPI1 promoter*-3X-HA-LUC-StrepII-FLAG digested by XbaI/NotI.

The pRS315-*LUC-PTC* plasmids were generated by overlap PCRs using a common outside primer pair, TPI1-promoter-F (PstI)/TPI13U-R (NotI), and an internal primer pair that introduced PTCs at specific codons: codon 20 (LUC-PTC20-F/R), codon 41 (LUC-PTC41-F/R), codon 160 (LUC-PTC160-F/R), codon 386 (LUC-PTC386-F/R), codon 460 (LUC-PTC460-F/R), and codon 520 (LUC-PTC520-F/R). In each case, the final PCR products were digested by PstI/NotI and cloned into pRS315 digested by PstI/NotI.

The pRS315-*PGK1* plasmid was constructed in four steps. First, a pRIP1 vector containing the *PGK1* promoter and 3′-UTR region (pRIP1-*PGK1 promoter-PGK1 3′-UTR*) was generated from pRIP1PGK1 (Peltz et al., 1993) by overlap PCRs using a common outside primer pair, M13-F/R, and a specific internal primer pair, PGK1-3U-F(BclI-NotI)/PGK1-pro-R(NotI-BclI). The final PCR products were digested by BamH1/HindIII and cloned into pRIP1PGK1 digested by BamH1/HindIII. Second, the *PGK1* coding region was amplified from pRIP1PGK1 by the primer pair PGK1-F-PciI/PGK1-R-XhoI, digested by PciI/XhoI, and ligated into pRS315-*LUC* previously digested by NcoI/XhoI, resulting in pRS315-*TPI1 promoter*-3X-HA-PGK1-StrepII-FLAG-*TPI1 3′-UTR*. Third, we generated pRIP1-*PGK1 promoter-HA-PGK1-SF-PGK1 3′UTR* by direct PCR. The PCR fragment was amplified from pRS315-*TPI1 promoter*-3X-HA-PGK1-StrepII-FLAG-*TPI1 3′-UTR* by the primer pair HA-F-BclI/SF-R-NotI, digested by BclI/NotI, ligated into pRIP1-*PGK1 promoter-PGK1 3′-UTR* digested by BclI/NotI. Fourth, a SmaI-HindIII fragment was isolated from pRIP1-*PGK1 promoter-HA-PGK1-SF-PGK1 3′UTR* and cloned into pRS315 digested by SmaI/HindIII.

The pRS315-*PGK1-PTCs* were generated by overlap PCR using a common outside primer pair, M13-F/M13-R, and an internal primer pair that introduced PTCs at specific codons: codon 37 (PGK1-PTC37-F/R), codon 84 (PGK1-PTC84-F/R), codon 219 (PGK1-PTC219-F/R), codon 309 (PGK1-PTC309-F/R). In each case, the final PCR products were digested by SmaI/HindIII and cloned into pRS315 digested by SmaI/HindIII.

pRS315 plasmids containing *LUC-PTC520-3U120, −3U200, −3U300, −3U400, −3U500,* and *-3U600* were all constructed by overlap PCRs in two steps. First, using a common outside primer pair (RS315-F-SalI/RS315-R-KasI) and a specific internal primer pair (3U120-F/3U120-R, 3U200-F/3U200-R, 3U300-F/3U300-R, 3U400-F/3U400-R, 3U500-F/3U500-R, and 3U600-F/3U600-R), we generated a set of pRS315 vectors with a *GAL7* polyadenylation signal (Bucheli et al., 2007) inserted at different locations of the 1 kb SalI-KasI fragment. Second, a PstI-XbaI fragment was isolated from pRS315-*LUC-PTC520* and ligated into this set of modified pRS315 vectors digested by PstI/XbaI. This set of *LUC-PTC520-xxUTR* alleles from pRS315 plasmids generates transcripts with 3′-UTR lengths ranging from 120 to 600 nt.

pRS316 plasmids containing *LUC* or *LUC-PTC* alleles were constructed in two steps. First, a HindIII-XbaI DNA fragment was isolated from the respective pRS315-*LUC* or *LUC-PTC* plasmids and cloned into pRS316. Then a XbaI-NotI fragment containing the *TPI1 3′* region was cloned downstream of the *LUC* or *LUC-PTC* ORF.

pRS315 derived plasmids were transformed into *upf1Δ* cells, and pRS316 derived plasmids were transformed into *pab1Δ pbp1Δ upf1Δ* or *pbp1Δ upf1Δ* cells, both by the high-efficiency method (Schiestl and Gietz, 1989).

Cell growth and western analysis

Cells were grown at 30°C in 25 mL of synthetic complete media lacking leucine or uracil to an optical density at 600nm (OD$_{600}$) of 0.7. For each culture expressing a specific *TPI1-PTC, LUC-PTC, PGK1-PTC*, or control allele, 10 OD$_{600}$ units were harvested for western analysis and 4 OD$_{600}$ units from the same culture were collected for RNA extraction. Cell pellets for western analyses were resuspended in 110 μl RIPA buffer (25 mM Tris-HCl pH 7.4, 150 mM NaCl, 1% NP-40, 1 mM EDTA, 5% glycerol) with 1mM PMSF and

1X protease inhibitor mixture (Thermo Scientific, #A32965). The cell suspensions were lysed by vortexing for 30 s with 0.1g pre-washed glass beads (Sigma-Aldrich, #8772), followed by 30 s on ice, for 8 cycles. The lysates were centrifuged at 12,000rpm for 15 min in a Sorvall Legend X1R centrifuge, at 4°C. Aliquots (90 μl) of the supernatants were mixed with Laemmli's SDS-sample buffer (Boston BioProducts, #BP-110R) followed by boiling for 5 min. The samples were then resolved by 10% SDS-PAGE, transferred to Immobilon-P membrane (Millipore, #IPVH0010), and incubated with anti-HA antibodies (Sigma-Aldrich, #H3663, 1:2,000), anti-FLAG antibodies (Sigma-Aldrich, #F7425, 1:1,000 or SANTA CRUZ, #sc-51590, 1:100), anti-Rps6 (Cell Signaling, #4858, 1:2,000), or anti-Pgk1 antibodies (Thermo Fisher, #459250, 1:4,000) overnight at 4°C. The membrane was washed with PBST for 7 min, 3 times, then incubated with anti-Mouse secondary antibodies (Thermo Fisher, #A24506, 1:5,000-1:10,000) or anti-Rabbit secondary antibodies (Sigma-Aldrich, #GENA934, 1:5,000) for 45 min at RT. Then the membrane was washed with PBST for 7 min, 3 times. Proteins were detected using ECL reagents and Hyperfilm ECL (GE, #28906835). The signal was analyzed with MultiGauge software.

Detection of peptidyl-tRNA
Peptidyl-tRNA was detected with *LUC-PTC20* and *LUC-PTC41* whole cell lysates. 35 OD600 units were harvested and resuspended in 250 μl RIPA buffer pretreated with RNasecure (Thermo Fisher, #AM7006) and supplemented with 1mM PMSF and 1X protease inhibitor. Cell lysates were then prepared as described above. To prepare cell lysates treated with cycloheximide, cells were incubated in the presence of cycloheximide (0.1mg/ml) for 5 min before harvest, and lysed in buffer supplemented with cycloheximide. To preserve peptidyl-tRNA ester linkage, cell lysates were denatured with Laemmli's sample buffer which was pretreated with RNasecure. To release the peptides, cell lysates were treated with 0.1 M NaOH for 5 min at 65°C, then neutralized with equimolar HCl. Samples were run without prior heat treatment on NuPAGE Bis-Tris gels with MES-SDS running buffer. To detect ^{35}S-fmet-tRNA^{fmet}, ^{35}S-fmet-tRNA^{fmet} molecules (a gift from Dr. A. Korostelev) were mixed with RNasecure treated Laemmli's sample buffer, run on NuPAGE Bis-Tris gels with MES-SDS running buffer, and detected by phosphorimaging using a Fujifilm bio-imaging analyzer (BAS-2500).

RNA preparation and northern analysis
Total RNA from cell pellets was isolated as described previously (Herrick et al., 1990). Briefly, pellets were resuspended in 500 μl buffer A (50 mM NaOAc pH5.2, 10 mM EDTA, 1% SDS, 1% DEPC), extracted with 500 μl RNA-phenol (phenol saturated with 50 mM NaOAc pH5.2, 10 mM EDTA) by vortexing for 10 s, followed by 50 s incubation in a 65°C water bath, for 6 cycles. Tubes were centrifuged at 12,000rpm in an Eppendorf 5417C centrifuge for 10 min at RT. The aqueous layers were recovered and followed by another phenol extraction. Phenol/chloroform (500 μl) was added to the recovered aqueous layer, and the mixture was vortexed for 2 min at RT followed by 10 min centrifugation at 12,000rpm. The aqueous layers were recovered and subjected to another phenol/chloroform extraction. The RNAs were precipitated by adding 40 μl NaOAc (3 M, pH 5.2) and 1 mL ethanol and incubated for 2 hours at −80°C. Tubes were centrifuged at 12,000rpm for 15 min at 4°C. Pellets were washed with 70% ethanol and re-dissolved in 50 μl RNase free distilled water. Aliquots (15 μg) of each RNA sample were loaded onto a 1% agarose/formaldehyde/MOPS gel and electrophoresed, blotted, and hybridized as described previously (He and Jacobson, 1995). Random-primed DNA probes made from NcoI-XbaI *LUC* fragments were used to detect *HA-LUC-SF* mRNAs, probes made from *StrepII-FLAG* fragments were used to detect *HA-TPI1-PTC-SF* and *HA-PGK1-PTC-SF* mRNAs, and full-length *SCR1* probes were used to detect the *SCR1* RNA (loading control). [α-^{32}P]-dCTP (Perkin Elmer, Blu513Z) and a random primed DNA labeling kit (Roche, # 11-004-760-001) were used to generate probes according to the manufacturer's protocol. Signals from Northern blots were detected and analyzed by phosphorimaging using a Fujifilm bio-imaging analyzer (BAS-2500) and MultiGauge software.

QUANTIFICATION AND STATISTICAL ANALYSIS

The following formulas were used to determine the relative efficiencies of PTC readthrough and termination:

$$Relative\ readthrough\ efficiency = \frac{\frac{FLAG}{Pgk1\ or\ Rps6}}{\frac{mRNA}{SCR1\ RNA}}$$

$$Relative\ termination\ efficiency = \frac{\frac{HA}{Pgk1\ or\ Rps6}}{\frac{mRNA}{SCR1\ RNA}}$$

In these formulas *FLAG, Pgk1, Rps6,* and *HA* respectively represent the amounts of full-length FLAG-tagged protein, Pgk1 protein, Rps6, and prematurely terminated HA-tagged protein determined by western blotting, and *mRNA* and *SCR1 RNA* respectively designate the levels of these two transcripts determined by Northern blotting. The results shown in the figures are the average of three independent experiments ± SEM unless otherwise indicated.